The Electronic States of the Tetrahedral Iron Clusters of Iron–Sulphur Proteins. A Theoretical Model

By **Andrew J. Thomson**, School of Chemical Sciences, University of East Anglia, Norwich NR4 7TJ

A simple molecular-orbital model is presented of the delocalised *d*-electron system of the polynuclear iron–sulphur clusters, $[Fe_4S_4(S\text{–}R)_4]^{n-}$ where n = 1, 2, or 3 and R = alkyl or aryl group, which are known to exist in certain proteins and as synthetic model compounds. The model separates, using symmetry arguments, the iron–sulphur and the iron–iron interactions leaving the final energy-level ordering to be established by experiment. It is shown that this model provides a reasonable interpretation of measured ground-state *g* factors of the paramagnetic oxidation states, where n = 1 or 3, of the cluster. The state where n = 2 is diamagnetic at low temperature. A closed-shell configuration is assigned to this oxidation level. This conclusion is at variance with that obtained from a SCF-Xα-SW calculation. Arguments are presented which reveal the inadequacy of the level scheme suggested by the Xα calculation.

THE presence of a polynuclear iron–sulphur cluster, $[Fe_4S_4(S\text{–}Cys)_4]^{n-}$ (where S–Cys is a cysteinyl residue in a polypeptide chain), consisting of an approximately tetrahedral array of four iron atoms, has now been recognised in a number of proteins.[1] This cluster can undergo

$$\underset{C^{3-}}{[Fe_4S_4(SR)_4]^{3-}} \rightleftharpoons \underset{C^{2-}}{[Fe_4S_4(SR)_4]^{2-}} \rightleftharpoons \underset{C^{-}}{[Fe_4S_4(SR)_4]^{-}} \quad (1)$$

one-electron redox changes as shown in equation (1).[2] The redox potentials are under control of the protein environment since no single protein is known which, in aqueous solution, will undergo reversible redox reactions between all three oxidation levels.[3] The C^{3-}–C^{2-} couple is found in many proteins extracted from bacteria such as *Bacillus stearothermophilus*, *Bacillus polymyxa*, *Clostridium pasteurianum*.[4] The redox change C^{2-}–C^{-} is found only in a protein from photosynthetic bacteria, notably *Chromatium*, which is termed high-potential iron protein (HP).[4]

A number of derivatives of this cluster having the general formula $[Fe_4S_4(S\text{–}R)_4]^{2-,3-}$, where R can be an alkyl or aryl group, have been prepared.[5] It has not yet proved possible to prepare a stable protein-free derivative of the C^{-} state.[6] A great deal of data that bear upon the question of the electronic structure of these centres has now been collected both on the model compounds and on the proteins. There are e.s.r.,[7] magnetic susceptibility,[8] Mössbauer,[4] optical, and magnetic circular dichroism [9–11] data on some of them. However, in spite of all the experimental evidence there is no wholly successful model of the electronic structures of these clusters. It is the purpose of this paper to report a simple molecular-orbital (m.o.) model which was suggested some years ago [12] and to suggest how experimental data might fit the model. Our conclusions are at variance with those drawn from other models in the literature.[13]

The clusters are mixed-valence [14] compounds which contain, in the case of the C^{2-} oxidation level, two iron(II) and two iron(III) ions. Therefore a description of the energy levels of the clusters can be made starting from either of two limits. If the coupling between the metal ions is weak compared with interelectronic repulsion and crystal-field splitting then the energy levels of isolated iron(II) and iron(III) ions are the natural starting point. The interaction between the metal ions is then introduced in the form of an extra term in the Hamiltonian of the type $\pm\sum_{i,j} J_{ij}S_iS_j$, representing exchange coupling. However, if the interaction between the metal ions is strong then it is more natural to use a molecular-orbital model in which orbitals are constructed from the four sets of atomic *d* orbitals on each metal centre. Metal electrons are then assigned to these delocalised orbitals.

The first model, more appropriate for valence-trapped clusters (class I in the Robin–Day scheme),[14] emphasises the localisation of metal electrons, whereas the second model stresses metal electron delocalisation and is more appropriate therefore for the description of valence-delocalised (class III A)[14] mixed-valence clusters. Appeal is made to experimental evidence to decide which of these two models is likely to be the more appropriate one.

Mössbauer spectroscopy has been applied widely to investigate the clusters both in proteins and in model compounds and is a valuable source of information on the question of the localisation of valences. The results on the clusters in the C^{2-} and C^{-} states are relatively straightforward.[4] Both in model compounds [15] and in protein bound clusters, the C^{2-} state consists of four equivalent iron atoms of average valence $Fe^{2.5+}$. The measured isomer shifts indicate this value. No inequivalence of the four atoms can be detected in the quadrupole splitting. The data on the C^{-} level clusters are limited because no models have yet been prepared and there are only a few protein examples known. The Mössbauer evidence on HP_{ox} (oxidised HP) from *Chromatium* shows a quadrupole split doublet at 77 K and 195 K.[16] Although it is not possible to resolve more than one pair of doublets, some broadening of the lines suggests slight inequivalence of the four iron atoms. However, it is not possible to make any distinction between the iron valences and an average valency of $Fe^{2.75+}$ has been assigned to the four iron atoms.[4] Mössbauer spectra measured in high magnetic fields reveal the presence of

positive and negative hyperfine fields which is indicative of some localisation of electron spin.[16] Presumably this excess of electron density on one or more iron atoms is not sufficient to show up in the quadrupole splitting. In the case of the C^{3-} state cluster the evidence is less clear cut. The Mössbauer spectrum of the reduced ferredoxin from *B. stearothermophilus* consists, at 77 K, of two pairs of quadrupole doublets with intensities in the ratio 1 : 1 and chemical shifts that indicate a slight difference between the valences of each pair of iron atoms.[17] However, in the reduced ferredoxin from *Cl. pasteurianum* the four iron atoms appear much more nearly equivalent and can be assigned as $Fe^{2.5+}$.[18] The Mössbauer spectra of a wide range of C^{3-} model compounds have been extensively investigated.[19] In frozen solution all the compounds show a pair of overlapping doublets with isomer shifts strikingly similar to those of the *B. stearothermophilus* protein. However, in the crystalline state the Mössbauer spectra are dependent both upon the cation and the ligand, S–R. Some compounds show two resolved pairs of doublets as in the solution phase whereas others give only a single pair of doublets similar to that seen in *Cl. pasteurianum* ferredoxin.

Hence, in conclusion, the Mössbauer spectra show that the iron atoms have, in the main, shared valences although some limited amount of spin localisation takes place and is more readily detectable in the paramagnetic oxidation states, C^{-} and C^{3-}. These results are in sharp contrast with the data on the two-iron ferredoxins in the reduced state. The Mössbauer data show two pairs of quadrupole doublets each with isomer shift and quadrupole splitting that is typical of a high-spin iron(III) and a high-spin iron(II) ion in a tetrahedral sulphur environment.[4] The presence of essentially iron(II) and iron(III) ions can also be confirmed by the near-i.r. optical spectrum in which bands have been located that can be assigned to the *d–d* states of pseudotetrahedral iron(II) and iron(III) ions.[10,20] Thus in the case of the two-iron centres there is little doubt that the coupling of the two-iron is a relatively weak perturbation compared with interelectronic repulsion and crystal-field effects.

By contrast the Fe_4S_4 cluster appears to be a largely valence-delocalised structure. Although some spin localisation is found which is dependent upon the oxidation level and the protein environment, the isomer shifts cannot be interpreted in terms of complete localisation as iron(II) and iron(III) ions. It is clearly of great interest to construct a molecular-orbital model of these clusters and to see how far it can account for the experimental data on their structural and electronic properties.

There have been published brief accounts of the molecular orbitals for tetrahedral metal clusters [21–23] but only with passing reference to the electronic structure of iron–sulphur clusters of biological importance. Few details have been given and no attempt has been made to match magnetic data to the model. The other theoretical model of interest is the SCF-Xα-SW calculation [13] for the C^{2-} oxidation state completed at the same time as our preliminary report of this present work. The ordering of energy levels obtained by the Xα method differs from that suggested by our work and a quite different ground-state electronic configuration is proposed.[13] The implications of the ground state proposed by the Xα calculation for the magnetic properties of the C^{-} and C^{3-} states was not explicitly considered.

THEORETICAL

Molecular-orbital Model.—The model used has previously been successfully employed to interpret the magnetic and optical properties of octahedral metal clusters.[24] Figure 1(*a*) is an idealised diagram of the cluster geometry.

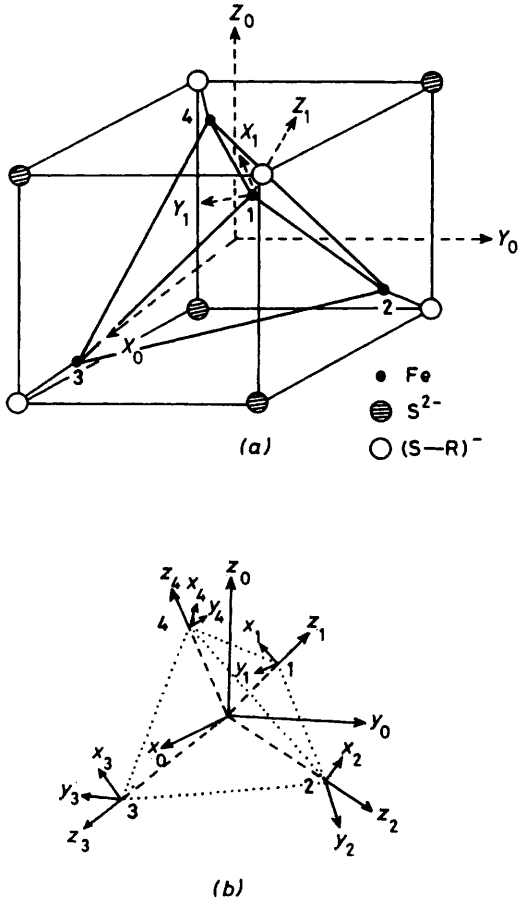

FIGURE 1 (*a*) Idealised diagram of cluster geometry showing numbering of iron atoms used and (*b*) the co-ordinate system employed

There are two types of interaction present which can be separated and left as semi-empirical adjustable parameters. The first is the iron–sulphur interaction due to the three S^{2-} ions and single $(S–R)^{-}$ group surrounding each iron atom. The second interaction arises from the metal–metal contact, which is *ca.* 2.776—2.732 Å in a dianion model complex.[25] Here these two interactions are separated as dictated by symmetry considerations and left as variable parameters since we have no satisfactory method of deciding their values *a priori*.

A set of local co-ordinates, x_n, y_n, and z_n, where $n = 1, 2, 3,$

or 4 numbers the iron atoms, are oriented about each atom as shown in Figure 1(*b*). The local z_n axis runs along the Fe–(S–R) bond. Assuming initially that the cluster is perfectly cubic, each iron atom experiences an identical local crystal field of C_{3v} symmetry due to the four sulphur ligands. Even if the influences of the other three iron atoms are considered, the local field remains C_{3v}.

The interaction between the metal atom and its four nearest neighbour sulphur ligands partially lifts the degeneracy of the *d* orbitals in the order: d_{xy}, $d_{x^2-y^2} < d_{xz}$, $d_{yz} < d_{z^2}$.

The *d* orbitals on each metal atom thus give rise to three subsets separated in energy by the local crystal field. Although this order is that predicted by a simple crystal-field model which ignores π bonding the order is not important at this stage. We intend to fix the order empirically at a later stage. The significance of this symmetry-determined separation of the *d* orbitals into subsets is that metal–metal bonding can be introduced by combining the orbitals from each subset only on each of the four metal atoms to generate LCAO m.o.s appropriate to the whole cluster. This procedure gives rise to more or less independent subsystems of m.o.s analogous in some respects to the σ–π separation commonly made for aromatic hydrocarbons. It is essentially the procedure introduced by Cotton and Haas [26] for metal clusters. The m.o.s formed in this way are found to transform according to (2)—(4) under the group T_d. The basis functions for these irreducible representations have been derived to be consistent with standard

$$(\sigma)\ d_{Z^2}: \quad a_1 + t_2 \qquad (2)$$

$$(\pi)\ d_{XZ},\ d_{YZ}: \quad e + t_1 + t_2 \qquad (3)$$

$$(\delta)\ d_{X^2-Y^2},\ d_{XY}: \quad e + t_1 + t_2 \qquad (4)$$

transformation relations [27] and are given, normalised, in Table 1.

TABLE 1

Molecular orbitals formed from subsets of *d* orbitals on four iron atoms transforming as irreducible representations under T_d.* Functions are normalised

$\lvert Z^2\rvert$		
a_1		$\frac{1}{2}[\theta_1 + \theta_2 + \theta_3 + \theta_4]$
t_2		$\frac{1}{2}[\theta_1 - \theta_2 - \theta_3 + \theta_4]$ $\frac{1}{2}[\theta_1 + \theta_2 - \theta_3 - \theta_4]$ $\frac{1}{2}[\theta_1 - \theta_2 + \theta_3 - \theta_4]$
$\lvert XZ,\ YZ\rvert$		
e	ϵ	$\frac{1}{2}[y_1z_1 - y_2z_2 - y_3z_3 + y_4z_4]$
	θ	$\frac{1}{2}[x_1z_1 - x_2z_2 - x_3z_3 + y_4z_4]$
t_1	Z	$\frac{1}{2}[y_1z_1 + y_2z_2 + y_3z_3 + y_4z_4]$
	X	$\frac{1}{4}[-y_1z_1 - y_2z_2 + y_3z_3 + y_4z_4]$ $+ \frac{\sqrt{3}}{4}[-x_1z_1 - x_2z_2 + x_3z_3 + x_4z_4]$
	Y	$\frac{1}{4}[-y_1z_1 + y_2z_2 - y_3z_3 + y_4z_4]$ $+ \frac{\sqrt{3}}{4}[x_1z_1 - x_2z_2 + x_3z_3 - x_4z_4]$
t_2	XY	$\frac{1}{2}[x_1z_1 + x_2z_2 + x_3z_3 + x_4z_4]$
	YZ	$\frac{1}{4}[x_1z_1 + x_2z_2 - x_3z_3 - x_4z_4]$ $+ \frac{\sqrt{3}}{4}[-y_1z_1 - y_2z_2 + y_3z_3 + y_4z_4]$
	XZ	$\frac{1}{4}[x_1z_1 - x_2z_2 + x_3z_3 - x_4z_4]$ $+ \frac{\sqrt{3}}{4}[y_1z_1 - y_2z_2 + y_3z_3 - y_4z_4]$
$\lvert X^2 - Y^2,\ XY\rvert$		
e	ϵ	$\frac{1}{2}[x_1y_1 + x_2y_2 + x_3y_3 + x_4y_4]$
	θ	$\frac{1}{2}[\xi_1 + \xi_2 + \xi_3 + \xi_4]$
t_1	Z	$\frac{1}{2}[x_1y_1 - x_2y_2 - x_3y_3 + x_4y_4]$
	X	$\frac{1}{4}[-x_1y_1 + x_2y_2 - x_3y_3 + x_4y_4]$ $+ \frac{\sqrt{3}}{4}[\xi_1 - \xi_2 + \xi_3 - \xi_4]$
	Y	$\frac{1}{4}[-x_1y_1 - x_2y_2 + x_3y_3 + x_4y_4]$ $+ \frac{\sqrt{3}}{4}[-\xi_1 - \xi_2 + \xi_3 + \xi_4]$
t_2	XY	$\frac{1}{2}[\xi_1 - \xi_2 - \xi_3 + \xi_4]$
	YZ	$\frac{1}{4}[-\xi_1 + \xi_2 - \xi_3 + \xi_4]$ $+ \frac{\sqrt{3}}{4}[-x_1y_1 + x_2y_2 - y_3x_3 + x_4y_4]$
	XZ	$\frac{1}{4}[-\xi_1 - \xi_2 + \xi_3 + \xi_4]$ $+ \frac{\sqrt{3}}{4}[x_1y_1 + x_2y_2 - x_3y_3 - x_4y_4]$

* $\theta_n \equiv z_n^2$ and $\xi_n \equiv x_n^2 - y_n^2$; Z, X, and Y, written as components of t_1 for convenience, denote the functions $Z(X^2 - Y^2)$, $X(Z^2 - Y^2)$, and $Y(Z^2 - X^2)$ respectively which form a basis for t_1 under T_d; $e\theta$ and $e\epsilon$ are the functions $3Z^2 - r^2$ and $X^2 - Y^2$ defined by Griffith (ref. 27).

The energies of these orbitals relative to the baricentres of the subsets can be calculated using a Hückel type of calculation. The m.o. energy is given by relation (5) where $\psi_n = \sum_{i=1}^{4} C_{ni}\phi_i$. The integral $H_{ii} = \langle\phi_i|H|\phi_i\rangle$ is taken as the unit of energy and, to a first approximation, is the

$$E_n = \langle\psi_n|H|\psi_n\rangle / \langle\psi_n|\psi_n\rangle \qquad (5)$$

same for all *d* orbitals ϕ. Off-diagonal elements are obtained from the approximation (6) where S_{ij} is the overlap integral $\langle\phi_i|\phi_j\rangle$.

$$H_{ij} = 2\,S_{ij}\,H_{ii} \qquad (6)$$

With these assumptions the m.o. energies, in units of H_{ii}, are given by the expressions in Table 2. In this Table the overlap integrals S_{ij} between adjacent atoms have been expressed in terms of the two-atom overlaps σ, π, and δ along the line joining the two atoms.

TABLE 2

Energies of the molecular orbitals of the subsets $\lvert Z^2\rvert$, $\lvert XZ,\ YZ\rvert$, and $\lvert X^2 - Y^2,\ XY\rvert$ in units of H_{ii}*

$\lvert Z^2\rvert$	
a_1	$\frac{2[2 + 3\,S(d\sigma, d\sigma) + 8\,S(d\pi, d\pi) + S(d\delta, d\delta)]}{[4 + 3\,S(d\sigma, d\sigma) + 8\,S(d\pi, d\pi) + S(d\delta, d\delta)]}$
t_2	$\frac{2[6 - 3\,S(d\sigma, d\sigma) - 8\,S(d\pi, d\pi) - S(d\delta, d\delta)]}{[12 - 3\,S(d\sigma, d\sigma) - 8\,S(d\pi, d\pi) - S(d\delta, d\delta)]}$
$\lvert XZ,\ YZ\rvert$	
e	$\frac{2[3 + 6\,S(d\sigma, d\sigma) - 5\,S(d\pi, d\pi) - S(d\delta, d\delta)]}{[6 + 6\,S(d\sigma, d\sigma) - 5\,S(d\pi, d\pi) - S(d\delta, d\delta)]}$
t_1	$\frac{2[1 - 2\,S(d\sigma, d\sigma) - S(d\pi, d\pi) - S(d\delta, d\delta)]}{[2 - 2\,S(d\sigma, d\sigma) - S(d\pi, d\pi) - S(d\delta, d\delta)]}$
t_2	$\frac{2[9 + 6\,S(d\sigma, d\sigma) + 19\,S(d\pi, d\pi) + 11\,S(d\delta, d\delta)]}{[18 + 6\,S(d\sigma, d\sigma) + 19\,S(d\pi, d\pi) + 11\,S(d\delta, d\delta)]}$
$\lvert XY,\ X^2 - Y^2\rvert$	
e	$\frac{2[12 + 3\,S(d\sigma, d\sigma) - 4\,S(d\pi, d\pi) + 2\,S(d\delta, d\delta)]}{[24 + 3\,S(d\sigma, d\sigma) - 4\,S(d\pi, d\pi) + S(d\delta, d\delta)]}$
t_1	$\frac{2[4 - S(d\sigma, d\sigma) - 4\,S(d\pi, d\pi) - 11\,S(d\delta, d\delta)]}{[8 - S(d\sigma, d\sigma) - 4\,S(d\pi, d\pi) - 11\,S(d\delta, d\delta)]}$
t_2	$\frac{[72 + 6\,S(d\sigma, d\sigma) + 88\,S(d\pi, d\pi) + 194\,S(d\delta, d\delta)]}{[72 + 3\,S(d\sigma, d\sigma) + 44\,S(d\pi, d\pi) + 97\,S(d\delta, d\delta)]}$

* $S(d\sigma, d\sigma)$, $S(d\pi, d\pi)$, and $S(d\delta, d\delta)$ are two-atom overlap integrals.

The next stage of the calculation involves mixing of m.o.s of like symmetry from different subsystems. However, this

second-order interaction depends only upon two-centre integrals and in practice is found to be small unless levels approach close to one another. In addition, the subsystems of m.o.s differ in energy by an unknown amount on the diagonal as a consequence of metal–ligand interaction. For these reasons we neglect this second-order mixing entirely. This neglect should be borne in mind when fitting experimental data to the model.

may be evaluated using Slater's rules. The value of $Z_{\text{eff.}}$ is 5.9 for Fe^0 and Fe^{II} and 6.25 for Fe^{III}. The maximum

$$\rho = Z_{\text{eff.}}R/3a_{\text{H}} \quad (7)$$

value of ρ, taking $R = 3$ Å and $Z_{\text{eff.}} = 6.25$, is therefore 11.8 and the minimum value, with $R = 2$ Å and $Z_{\text{eff.}} = 5.90$, is 7.4.

On this basis the energy-level diagram of Figure 2 was

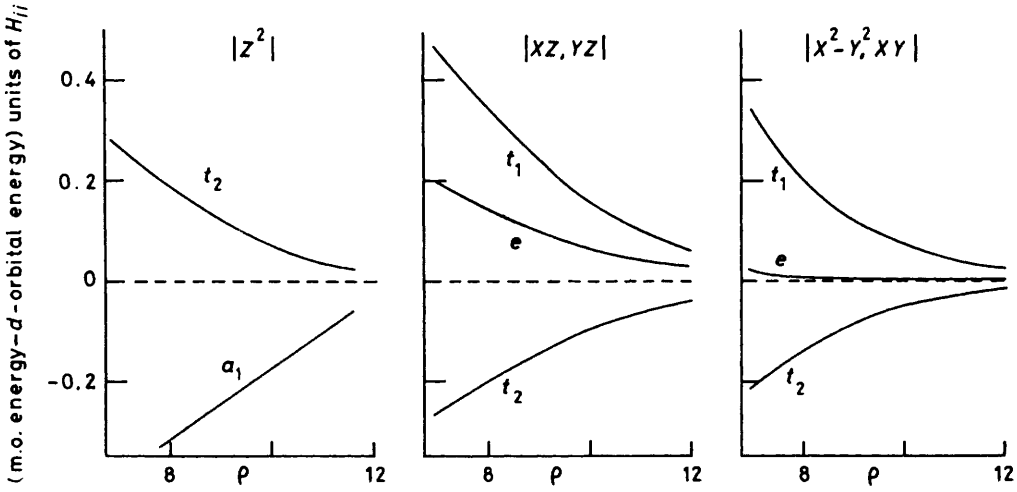

FIGURE 2 Energy-level diagram for the cluster $[Fe_4S_4(S{-}R)_4]^{2-}$. Each *d*-orbital subsystem is shown separately. $\rho = \alpha R$, where α is the Slater orbital exponent and R is the metal–metal distance. The point group assumed is T_d

The evaluation of the m.o. energies requires the assumption of wavefunctions for the metal *d* orbitals. In view of the approximations already inherent in the calculation we use simple Slater 3*d* orbitals. The large internuclear distance of *ca.* 2.8 Å between the metal atoms makes it likely that Slater orbitals are a reasonable approximation to the true wavefunctions in the region of large overlap. The m.o. energies have been evaluated as a function of a single parameter ρ, equal to αR where α is the orbital exponent and R the metal–metal distance. The overlap integrals have been obtained from standard tables. The range of values of ρ selected is 7.0—12.0. This range was chosen using relation (7) and $Z_{\text{eff.}} = Z - S$ where Z is the atomic number of the element and S, the screening constant, which obtained. Each subsystem is shown separately. The ordering of the energy zeros is probably d_{XY}, $d_{X^2-Y^2} < d_{XZ}$, $d_{YZ} < d_{Z^2}$ but this is not implied in Figure 2.

Electronic Configuration.—In order to establish the electronic configurations of the ground states of the three accessible oxidation levels of the cluster, appeal is made to the experimentally determined magnetic properties. Table 3 summarises the facts for these oxidation states. A formal count of all the *d* electrons leads to 21, 22, and 23 electrons for the states C^-, C^{2-}, and C^{3-} respectively.

There is only one well characterised example of the C^- state, namely HP_{ox}.

The e.s.r. spectrum is complex, consisting of two sets of *g* factors, an axial pair with $g_{\parallel} = 2.120$ and $g_{\perp} = 2.040$ and

TABLE 3

Comparison of the electronic configurations of the three accessible oxidation states of $[Fe_4S_4(S{-}R)_4]^{n-}$ clusters

Examples	C^- ($n = 1$) HP_{ox}	C^{2-} ($n = 2$) HP_{red} Oxidised *Cl. pasteurianum* ferredoxin $[Fe_4S_4(SCH_2Ph)_4]^{2-}$	C^{3-} ($n = 3$) Super-reduced HP Reduced *Cl. pasteurianum* ferredoxin $[Fe_4S_4(SCH_2Ph)_4]^{3-}$
Formal oxidation states of metal ions	$1Fe^{II} + 3Fe^{III}$	$2Fe^{II} + 2Fe^{III}$	$3Fe^{II} + 1Fe^{III}$
Number of electrons	21	22	23
g Factors	$g_{\parallel} = 2.120$ $g_{\perp} = 2.040$ $g_1 = 2.087$ $g_2 = 2.055$ $g_3 = 2.040$	*a*	$g_z = 2.07$ $g_y = 1.93$ *b* $g_x = 1.89$ $g_{\parallel} = 2.04$ $g_{\perp} = 1.93$ *c*
Electronic configuration of highest filled orbitals	$e^3\,t_1^0$ or $e^3\,e^0$	$e^4\,t_1^0$ or $e^4\,e^0$	$e^4\,t_1^1$ or $e^4\,e^1$

[a] $\mu_{\text{eff.}}$ (at 220 °C) of the metal ion is in the range 0.90—1.24 B.M. Diamagnetic at low temperature. [b] Values for half-reduced *Cl. pasteurianum* ferredoxin and *B. stearothermophilus*. [c] Values for super-reduced HP in dimethyl sulphoxide and $[Fe_4S_4(SCH_2Ph)_4]^{3-}$.

a rhombic set with $g_1 = 2.087$, $g_2 = 2.055$, and $g_3 = 2.040$.[8] The different relaxation rates and saturation characteristics taken together with the chemical homogeneity of the protein led the authors to conclude that there was slow exchange of a single electron between iron sites within a single cluster. However, in this paper we examine whether these g factors can be interpreted satisfactorily within the framework of a fully delocalised model. We merely point out at this stage that both sets of g values are just *above* the free electron value. The C^{2-} state is diamagnetic at low temperature.[8] This implies a closed-shell configuration for this state. However there is thermal accessibility of a low-lying level at room temperature.[8,28] In the fully reduced state, C^{3-}, an e.s.r. signal is again detectable. The model compounds [29] and super-reduced HP,[3] from which the influence of the protein has presumably been removed, give axial g factors with $g_{av.}$ *below* the free electron value. The influence of the protein in a native compound produces a rhombic spectrum.[30] It is natural to suppose that on reduction of the C^{2-} state to C^{3-} the extra electron goes into the low-lying orbital which was thermally accessible at room temperature in C^{2-} state compounds.

These facts point to the involvement of two energy levels in the way suggested at the bottom of Table 3. The pattern of filling shown accounts for the above properties in the following way. The C^- state possesses a highest filled orbital of e symmetry which is more than half full. An orbital of this symmetry under T_d has no first-order orbital moment. Therefore the orbital contribution to the g value arises from the mixing, *via* spin–orbit coupling, of an excited state with an orbital moment. Furthermore, since the e shell is more than half full this contribution will be in a positive sense giving g values *above* 2.00. The situation is quite analogous to that seen in monomeric copper(II) compounds, with electronic configurations of $t_2^6e^3$ and g values above 2.00.[31] Addition of an electron closes the e shell and results in the diamagnetic C^{2-} state. Further reduction to C^{3-} places a single electron in the next highest orbital. If this were an e orbital or a t orbital with a quenched first-order orbital moment, a g factor just below the spin-only value will result since the shell will be less than half full and the orbital contribution mixed in by spin–orbit coupling will be in a negative sense. It is possible that an orbital of t symmetry contains the single electron since metal complexes such as $[Ti(acac)_3]$ (acac = acetylacetonate) with the configuration t_2^1 give g factors of $g_{\|} = 2.000$ and $g_{\perp} = 1.921$ [31] surprisingly close to those seen in the C^{3-} state.

Our argument is based upon the assumption that there is no gross re-ordering of energy levels on change of oxidation state. However, this assumption can only be justified finally by the satisfactory fitting of data to the model and by a successful tracking of changes in the optical spectrum on oxidation or reduction.

With this pattern in mind the energy levels of Figure 2 must be filled with 22 electrons to produce a closed shell. If the separation of the energies of the subsystem is ignored, that is, we assume that the metal–metal interaction is large compared with the metal–sulphur interaction, the first 18 electrons can be added with no choice to give the configuration at all values of ρ, $a_1^2 < t_2^6 \sim t_2^6 < e|XY, X^2 - Y^2|^4$. Above these levels are three, $e|XZ, YZ|$, $t_2|Z^2|$, and $t_1|XY, X^2 - Y^2|$, close together in energy at high ρ but with $e|XZ, YZ|$ being lowest at low ρ. Placing the remaining four electrons into $e|XZ, YZ|$ will produce the required closed-shell configuration with 22 electrons and the following ordering: $a_1^2 < t_2^6 \sim t_2^6 < e|XY, X^2 - Y^2|^4 < e|XZ, YZ|^4$.

It might have been supposed that the highest filled orbital could be of e symmetry derived from the splitting of one of the t orbitals by an axial distortion, from T_d to D_{2d}, of the cluster to give an a and e orbital.[13] But we reject this possibility since an e orbital thus formed will have an orbital moment. Hence the g factors of the C^- state will be difficult to reconcile with this scheme.

We have also considered the possibility that the $|Z^2|$ subsystem is pushed to very high energy by the repulsion due to the $(S-R)^-$ groups pointing directly along the local z_n axes. If the strongly bonding $a_1|Z^2|$ orbital is removed from amongst the occupied set then a closed-shell 22-electron configuration is only possible as follows: $t_2^6 \sim t_2^6 < e|XY, X^2 - Y^2|^4 < t_1|XY, X^2 - Y^2|^6$. Again it turns out that a satisfactory fit of the g factors of the C^- state with a configuration of t_1^5 cannot be obtained. We therefore discard this level ordering also.

It must be admitted that a number of energy-level ordering schemes compatible with the magnetic data are possible. However, the value of the model is that it severely restricts the choice. We have selected the following energy-level scheme (8) as the one giving the best fit of the data and in

$$a_1|Z^2|^2 < t_2|XZ, YZ|^6 \sim t_2|XY, X^2-Y^2|^6 < e|XY, X^2-Y^2|^4 < e|XZ, YZ|^4 < t_1|XY, X^2-Y^2|^0 \quad (8)$$

the following section show how this can be made to interpret the g factors reasonably quantitatively.

Estimate of g *Factors.*—C^- *State.* According to qualitative arguments made in the last section the cluster in the C^- state possesses the electronic configuration $e|XY, YZ|^3$ giving ^2E as the ground state. We follow closely the method outlined for copper(II) complexes by Griffith.[32]

The ground state is split by spin–orbit coupling and a tetragonal field, the resulting states transforming as the representations E' and E'' of the spinor group D_{2d}^*. Under the influence of second-order spin–orbit coupling, excited states carrying orbital angular momentum are mixed to provide the deviation from the spin-only g value. A rather large number of excited states are predicted to arise from the various possible electronic configurations. Thus there are two excited configurations e^2t_1, where t_1 is either $t_1|XY, X^2 - Y^2|$ or $t_1|XZ, YZ|$. Each of these configurations gives rise to five states, namely, $^4T_2$, $2\ ^2T_1$, $2\ ^2T_2$. The two other excited configurations which will carry a first-order orbital moment are $e^4t_2^5$ where t_2 is either $t_2|XZ, YZ|$ or $t_2|XY, X^2 - Y^2|$. These two configurations give rise to only two excited states, both $^2T_2$. Under the point group D_{2d} all of these excited states are potentially able to mix with the ground state *via* second-order spin–orbit coupling. The contribution of any one state is inversely proportional to its energy separation from the ground state. Therefore a detailed knowledge and assignment of the low-lying excited states of HP_{ox} is required before a definitive calculation can be undertaken.

We show here a specimen calculation to illustrate the contributions of the excited $^2T_2$ states, arising from the configurations $e^4t_2^5$, to the ground-state g factor.

Under D_{2d} the $^2T_2$ states of T_d become classified as ^2E and $^2B_2$ leading to the spinor representations E'', E' and E'' respectively.

The two possible ground-state wavefunctions can be written as (9) and (10). The symbols $|\xi_1\rangle, |\pm 1\rangle$ represent

the complex components of either t_2 orbital. The coefficients C_{1-6} are all of the form (11) where $\mathscr{H}_{SO}$ is the Hamiltonian of spin–orbit coupling and Δ is the energy

$$|E'\,\alpha'\rangle = |\theta^+\rangle - C_1|1^-\rangle$$
$$|E'\,\beta'\rangle = |\theta^-\rangle - C_2|-1^+\rangle \quad (9)$$

$$|E''\,\alpha''\rangle = |\varepsilon^+\rangle - C_3|\xi_1{}^+\rangle - C_4|-1^-\rangle$$
$$|E''\,\beta''\rangle = |\varepsilon^-\rangle - C_5|\xi_1{}^-\rangle - C_6|1^+\rangle \quad (10)$$

$$C_1 = \langle 1^-|\mathscr{H}_{SO}|\theta^+\rangle/\Delta \quad (11)$$

separation between the ^2E ground state and the $^2T_2$ excited state. It is assumed that the tetragonal splitting of both ^2E and $^2T_2$ is small compared with the separation between the baricentres of the states.

The coefficients C_{1-6} have been evaluated and are given in Table 4. Substitution of these values into the equation for

TABLE 4

Coefficients of second-order spin–orbit coupling between ^2E and two $^2T_2$ states in units of $\hbar^2\xi$, where ξ is the spin–orbit coupling constant for the e^3 configuration. Δ' is the energy separation between ^2E and $^2T_2|XZ, YZ|$ and Δ'' between ^2E and $^2T_2|XY, X^2 - Y^2|$

	$^2T_2\|XY, X^2 - Y^2\|$	$^2T_2\|XZ, YZ\|$
C_1, C_2	$-\frac{1}{2\Delta''}$	$-\frac{1}{2\sqrt{2}\Delta'}$
C_3, C_5	$-\frac{1}{\sqrt{6}\Delta''}$	$-\frac{1}{2\sqrt{3}\Delta'}$
C_4, C_6	$-\frac{1}{2\sqrt{3}\Delta''}$	$-\frac{1}{2\sqrt{6}\Delta'}$

the wavefunctions of E' and E'' allows evaluation of $g_\parallel$ and $g_\perp$ using equations (12.47) of Griffiths [32] and the matrix elements of L calculated in the Appendix. The following results, equations (12) and (13), are obtained. It is instructive to compare these results with the values obtained by

E'

$$g_\parallel = 2.0$$
$$g_\perp = 2.0 + \tfrac{1}{2}\frac{\xi}{\Delta'} \quad t_2|XZ, YZ|$$
$$g_\perp = 2.0 + \frac{\xi}{\Delta''} \quad t_2|XY, X^2 - Y^2| \quad (12)$$

E''

$$g_\parallel = 2.0 + \tfrac{2}{3}\frac{\xi}{\Delta'} \quad t_2|XZ, YZ|$$
$$g_\perp = 2.0 + \tfrac{1}{6}\frac{\xi}{\Delta'}$$
$$g_\parallel = 2.0 + \tfrac{4}{3}\frac{\xi}{\Delta''} \quad t_2|XY, X^2 - Y^2|$$
$$g_\perp = 2.0 + \tfrac{1}{3}\frac{\xi}{\Delta''} \quad (13)$$

Griffith,[32] equation (12.50), for tetragonally distorted copper(II) compounds. Using our notation his expressions become those of (14) and (15). Note that E' and E'' are the

$$E''\ g_\parallel = 2.0 \text{ and } g_\perp = 2.0 + 6\frac{\xi}{\Delta} \quad (14)$$

$$E'\ g_\parallel = 2.0 + 8\frac{\xi}{\Delta} \text{ and } g_\perp = 2.0 + 2\frac{\xi}{\Delta} \quad (15)$$

spinor representations of the group $D_4{}^*$ in this case but are for $D_{2d}{}^*$ in the former case.

In the case of the clusters, the contributions to the g factors from the orbital moments of $^2T_2|XY, X^2 - Y^2|$ and $^2T_2|XZ, YZ|$ are exactly $\frac{1}{3}$ and $\frac{1}{6}$, respectively, of the copper(II) values for equal magnitudes of the spin–orbit coupling constant and energy separation.

We now turn to a consideration of whether these results are capable of interpreting the complex e.s.r. patterns found in HP_{ox}.[8] First it is pertinent to consider the e.s.r. signals of octahedral copper(II) compounds which also possess a ^2E state. Many of them display interesting temperature-dependent properties. Typical of these results is the first example to be thoroughly studied, $Cu_3Bi_2(NO_3)_{12}\cdot 2H_2O$.[33] This compound gives an e.s.r. spectrum at 90 K which is almost isotropic ($g_\parallel = 2.219 \pm 0.003$, $g_\perp = 2.217 \pm 0.003$) but at 20 K a static distortion is frozen in resulting in an axial spectrum ($g_\parallel = 2.454 \pm 0.003$, $g_\perp = 2.096 \pm 0.003$). This and other examples [34] are interpreted in terms of a dynamic Jahn–Teller distortion at high temperature giving rise to the isotropic spectrum but with a static distortion which freezes in at low temperature. In the case of $Cu[BrO_3]_2\cdot 6H_2O$ several anisotropic spectra are observed at 20 K.[31] The reason why the copper(II) ion displays this effect in a number of its compounds is that the ^2E state has no first-order orbital moment, effectively $L = 0$, therefore spin–orbit splitting of this state is small and cannot stabilise the structure against a Jahn–Teller distortion.

Arguments have been presented in this paper that the electronic ground state of HP_{ox} is ^2E. Therefore consideration must be given to an interpretation of the e.s.r. spectrum of HP_{ox} in terms of the freezing in of two species at low temperature. Distortion of the tetrahedral ^2E state due to the Jahn–Teller effect occurs by the coupling with an ε vibrational mode and is expected to lead to a D_{2d} or D_2 structure in the absence of steric restraints from the environment. The tetrahedron may distort either by elongation or compression along its S_4 axis. The ground state observed at low temperature will therefore be either E' or E'' depending upon the distortion undergone. If, on freezing, the cluster populates each state then two species could be observed *via* e.s.r. spectroscopy at low temperature. At room temperature the clusters will become identical and therefore the protein will be chemically homogeneous. Furthermore, the average geometry as detected by X-ray crystallography should be close to tetrahedral.

The axial pair of g factors with $g_\parallel = 2.12$ and $g_\perp = 2.04$ are well accounted for by our model if they arise from a cluster with the E'' ground state. The expressions, equation (13), deduced predict the orbital contribution to $g_\parallel$ to be four times that of $g_\perp$. The experimental result is three times. If the contribution from the $^2T_2|XY, X^2 - Y^2|$ state dominates then we put $\frac{4}{3}\frac{\xi}{\Delta'}$ equal to 0.12. The free-ion value of ξ for iron is 410 cm^{-1} but allowing for orbital reduction a value of 300 cm^{-1} is reasonable. This indicates a value of 3 000 cm^{-1} for Δ'. Thus the g values require an excited state between *ca.* 2 000 and *ca.* 4 000 cm^{-1}. If other excited states contribute to the orbital moment then a larger value of Δ' is implied. Magnetic circular dichroism (m.c.d.) and c.d. measurements have revealed electronic states extending as low as 5 000 cm^{-1} in the optical spectrum of HP_{ox}.[10] Measurements to lower energy have not been possible on account of the intense i.r. absorption from the protein. The significance of the small values of the coefficients C_{1-6} referred to earlier is now apparent since the smaller they are the lower the value of Δ' is predicted to be.

This is in qualitative accord with the observation of numerous low-energy electronic states in the optical spectrum.

The other state, E', which could be frozen in is expected to belong to an axially distorted tetrahedron, at least in the absence of external steric constraints, with g values given by equation (12). The observed values are a rhombic trio. It is possible that this further lowering of symmetry arises from the protein constraints. The calculation of a rhombic spectrum is not likely to be a useful exercise since the number of parameters required increases rapidly.

C^{3-} *State.* The electronic configuration is taken to be $t_1|XY, X^2 - Y^2|^1$. As the g factors are anisotropic, see Table 1, the symmetry is lower than T_d. The model compounds give axial and the proteins rhombic spectra. We show here that it is possible for an axial model, with D_{2d} symmetry, to yield g factors close to those observed with the electronic configuration suggested.

Again we follow closely the treatment given by Griffith [32] for a d^1 tetragonally distorted titanium(III) complex. It is shown in the Appendix that the matrix elements of L_z within the $t_1|XY, X^2 - Y^2|$ manifold give an orbital angular momentum of $\pm \hbar$. This is identical with the orbital moment of a $^2T_2$ state arising from the configuration d^1. Thus the treatment needed is identical with that of Griffith and his expressions, equations (12.57)—(12.60),[27] are valid.

Under the group D_{2d}, $^2T_1$ of the tetrahedron splits into $^2A_2$ and ^2E. The separation between them is δ. Spin–orbit interaction yields a Kramers doublet E' from $^2A_2$ and two doublets, E' and E'', from ^2E. Note that these spinor representations E' and E'' correspond to E'' and E', respectively, of D_4* as used by Griffith.[27] E'' cannot be the ground doublet. It has g factors close to zero, as it arises from the $J = \pm \frac{3}{2}$ level. However, for E' we have equations (16).

$$\begin{aligned} g_{\|} &= -1 + 3S^{-1}(\delta + \tfrac{1}{2}\xi) \\ g_{\perp} &= 1 + S^{-1}(\delta - \tfrac{3}{2}\xi) \\ S &= (\delta^2 + \xi\delta + \tfrac{9}{4}\xi^2)^{\frac{1}{2}} \end{aligned} \qquad (16)$$

Griffith states that the only way $g_{\|}$ can be near 2.0 as observed is for ξ/δ to be small. In this case $g_{\perp} = 2 - (2\xi/\delta)$. Since experimentally $g_{\perp} = 1.93$, $\xi/\delta \approx 0.035$. If $\xi = 350$ cm^{-1} then $\delta = 10\,000$ cm^{-1}, or if $\xi = 250$ cm^{-1}, $\delta = 7\,000$ cm^{-1}. This is a large tetragonal splitting of the $^2T_1$ state but it has been observed for titanium tris(acetylacetonate), which possesses a trigonal perturbation.[31]

A contribution to $g_{\|}$ can come from an excited state transforming as $^2A_1$ under D_{2d}, of ^2E tetrahedral parentage. The expression for $g_{\|}$ is $2 + \lambda(\xi/\delta')$ where δ' is the energy separation between the $^2A_2$ ground state and $^2A_1$ and λ is the coefficient of second-order spin–orbit mixing. The value of λ will depend upon the nature of the state $^2A_1$ although this contribution to $g_{\|}$ must enter with the opposite sign to that for $g_{\perp}$. The observed value of $g_{\|}$ is 2.04 for the model compounds, above the free electron value.

Excited electronic states have been detected in C^{3-} state proteins at energies down to 5 000 cm^{-1} by m.c.d. and c.d. spectroscopy.[10] This model requires that there be such low-lying states. No detailed assignment has yet been made.

C^{2-} *State.* The model makes a basic assumption that the electronic levels are not grossly changed in energy as the oxidation level of the cluster alters. This assumption can only be justified finally by the success of the model in rationalising as many electronic properties as possible. It may prove possible to track changes in the energy levels on oxidation by observation of the optical properties of the clusters. This requires optical data, especially m.c.d. spectra, over as wide an energy range as possible and at low temperatures for clusters in all these accessible oxidation states. Collection of these data has begun.[9-11]

The preceding arguments imply that the electronic configuration of the C^{2-} state is $e|XY, YZ|^4\, t_1|XY, X^2 - Y^2|^0$ and hence diamagnetic. However, there can be excited states $^{1,3}T_1$ and $^{1,3}T_2$ arising from the configuration $e^3t_1^1$. If one or more of these states lies close to the ground state then it can be thermally populated to give a temperature-dependent paramagnetic moment.

The evidence both from model compounds and from the reduced form of *Chromatium* HP is that the C^{2-} cluster is diamagnetic at temperatures below 100 K.[8,25,28] At temperatures above this the magnetic moment per iron atom of the model compound $[NEt_4]_2[Fe_4S_4(SCH_2Ph)_4]$ rises to 1.04 B.M.* at 296 K.[35] There is disagreement about the magnitude of the paramagnetic moment of HP_{red} (reduced HP) at temperatures above 100 K. One report [28] gives a value of 0.6 B.M. per iron atom at 150 K, whilst a more recent study [8] fails to find appreciable population of a paramagnetic state up to 240 K. However, susceptibility data on proteins are notoriously sensitive to traces of iron impurity especially when small magnetic moments are being sought. More convincing evidence for a small paramagnetic moment at room temperature in a protein-bound C^{2-} cluster is given by the observation of contact-shifted proton resonances with a positive temperature dependence in the n.m.r. spectrum.[36]

The presence of a temperature-dependent paramagnetic moment implies only that there are low-lying paramagnetic electronic states which are thermally accessible. It is often taken to imply the presence of antiferromagnetic coupling. However, the mere detection of low-lying electronic states gives no information about their origin, that is, whether they arise from a ladder of exchange-coupled states or from excited electronic configurations.

DISCUSSION

The molecular-orbital model presented here was constructed in order to provide an energy-level scheme against which the optical and low-temperature m.c.d. spectra of four-iron sulphur clusters might be understood. It is deliberately empirical so that experimental data may be fed in. Since the clusters contain a large number of valence electrons it is difficult to have total confidence in *ab initio* calculations of the electronic energy levels of these systems. Instead the magnetic data, especially g factors, have been used in order to establish the electronic configurations of the ground states. The anisotropy of the g factors depends upon the character of low-lying excited electronic states and therefore must be consistent with the optical data.

Although the model presented starts with the picture of a fully delocalised d-electron system for all three oxidation levels it is possible to accommodate limited inequivalence of the atoms rather readily. Distortion of the tetrahedral metal cluster along, say, a three-fold axis through an iron atom to produce a C_{3v} array makes one iron atom inequivalent to the other three. The way in

* Throughout this paper: 1 B.M. = 9.274×10^{-24} A m^2.

which molecular-orbital degeneracies are lifted by this distortion is readily determined by symmetry theory. This would also be reflected, as shown earlier, in the anisotropies of g factors and possibly also in the splitting of electronic absorption bands if the distortions were large enough. An inequivalence may also be observed in Mössbauer and n.m.r. experiments. However, these experiments are very sensitive to small degrees of localisation of electron-spin density. Such properties are not readily calculated by an m.o. method. It is for this reason that models built upon Mössbauer data invariably take as their starting point a valence localised model into which exchange coupling is introduced. But in order to produce the extent of delocalisation suggested by the Mössbauer isomer shifts it is necessary to envisage an exchange coupling comparable in magnitude to or greater than interelectronic repulsion. In this case perturbation theory is no longer a valid approximation to determine energy levels. Hence, in our view, it will never be possible to produce a realistic model of the electronic structures of the four iron clusters starting from a localised valence viewpoint with the subsequent introduction of antiferromagnetic coupling. It is as inappropriate to speak of these clusters as antiferromagnetically coupled as it is to describe the structure of the hydrogen molecule as a pair of antiferromagnetically coupled hydrogen atoms.

The SCF-Xα-SW calculation agrees with the molecular-orbital model in assigning 22 electrons to fully delocalised orbitals which are mainly Fe in character.[13] However, the assignment of the highest occupied orbital disagrees completely with that proposed here in order to interpret the e.s.r. properties of the clusters. The Xα model proposes that the high occupied orbital in the C^{2-} state transforms as t_2 under T_d, and contains four electrons. The states which arise from the configuration t_2^4 are $^3T_1$, $^1A_1$, ^1E, and $^1T_2$. The triplet state is expected to be lowest according to Hund's rule. In order to account for the observed diamagnetism of the C^{2-} state at low temperature a Jahn–Teller distortion has been invoked, which, so it is claimed, will split the energy of the t_2 orbital into two sub-levels e and b_2.[37] The resulting electronic configuration e^4 is then diamagnetic. However, this is an erroneous argument. The effect of a Jahn–Teller distortion operating *via* an ε mode upon a state $^3T_1$ is to give two states ^3E and $^3B_2$. The term in the Hamiltonian which represents the Jahn–Teller effect only operates on orbital space since it is a vibronic operator. Therefore the spin of the state is unaffected by a Jahn–Teller distortion. In order for the spin state to be changed by the operation of the Jahn–Teller effect it is necessary for the effect to be greater in magnitude than the interelectronic repulsion which separates the triplet state from the lowest singlet state. There is no well substantiated example in the literature of a Jahn–Teller effect which leads to a spin crossover.[37] It is possible that the D_{2d} distortion commonly observed in pseudo-tetrahedral metal clusters leads to a crystal-field splitting sufficiently large to bring a component of one of the singlet states below those of the triplet. But this seems unlikely. Thus it is not valid to invoke the Jahn–Teller effect as the cause of the D_{2d} distortion or the source of the low-temperature diamagnetism.

The electronic configuration proposed on the basis of the Xα calculation is unsatisfactory in another respect.[13] It fails to predict the correct magnetic properties for the C^- and C^{3-} states. No Xα calculations specifically for these oxidation levels have been published. However, it must be supposed that the C^- state will have the electronic configuration t_2^3 if no gross re-ordering of levels takes place on oxidation. The states which arise from this configuration are $^4A_2$, ^2E, $^2T_1$, $^2T_2$. The ground state is therefore predicted by the Xα method to be $^4A_2$. However, this is quite at odds with the data from several types of experiment. First, the g factors determined are very close to 2.0. This can only arise for the $^4A_2$ state if zero-field splittings are virtually zero. Secondly, the magnetic moment of oxidised HP is *ca.* 2.00 B.M., which is far from the value of 3.9 B.M., the spin-only value expected for a $S = \frac{3}{2}$ state.[8] Finally, recent m.c.d. magnetisation curves of oxidised HP are consistent with an $S = \frac{1}{2}$ state and quite inconsistent with a ground state of $S = \frac{3}{2}$.[11]

For the C^{3-} oxidation level the Xα model predicts a configuration t_1^5 which leads to a single state $^2T_1$. This state will have a first-order orbital moment unless it is quenched by a distortion. However, the deviation of the orbital moment will be in the positive sense so as to give an average g value *greater* than 2.00, not as observed experimentally *lower* than 2.00.[27]

In constructing a semi-empirical m.o. model we have had in mind the fitting together of a large body of experimental data, especially magnetic experiments, from different oxidation levels. Furthermore, such a model does lend itself to the computation of the angular momentum properties of electronic states. Techniques such as e.s.r., m.c.d. spectroscopy, and magnetic susceptibility measure quantities which are sensitive to these properties and hence this is a suitable model. The Xα technique does not apparently lend itself readily to the computation of these quantities. However, no prediction can be made from m.o. models of molecular shape. Much has been made of the role of the Jahn–Teller effect in accounting for deviations of tetrahedral clusters from ideal T_d symmetry. We have argued here that the role of the Jahn–Teller effect has been incorrectly invoked. We take it as no criticism of our model that it proposes a closed-shell configuration for the C^{2-} oxidation level although it is distorted by a compression along the S_4 axis to give a D_{2d} molecule. There are many examples of closed-shell molecules which do not adopt a regular geometry.[38] It is not necessary to invoke the Jahn–Teller effect whenever a distorted structure is discovered.

We have, however, invoked the Jahn–Teller effect to re-interpret the unusually complex e.s.r. spectra of oxidised HP and have suggested that at very low temperature the cluster freezes into one of the two potential surfaces, presumably with equal probabilities. One

consequence of this explanation is that the e.s.r. spectrum of HP_{ox} should become isotropic at high temperature, the exact temperature depending upon the magnitude of the Jahn–Teller effect. Unfortunately the e.s.r. spectrum is not detectable above about 40 K as line widths become too broad. This rapid increase in the relaxation rate is due to the presence of low-energy electronic states. A further corollary is the prediction that the structure of HP_{ox} should average to a perfect tetrahedron at room temperature but should freeze into one of two differently distorted shapes at low temperature. *X*-Ray studies on HP indeed show that, on oxidation of the cluster, the shape changes from a tetrahedron with an appreciable tetragonal distortion to one of more nearly tetrahedral shape. However, it must be acknowledged that neither this hypothesis nor the rather elaborate electron hopping scheme suggested by Antanaitis and Moss [8] are totally satisfactory. Although the e.s.r. spectrum of HP_{ox} from *Chromatium vinosum* is complex, consisting of two species with different saturation characteristics, the e.s.r. spectrum of HP_{ox} from *Rhodopseudomonas gelatinosa* [39] gives a simple axial signal with $g_{\|} = 2.11$ and $g_{\perp} = 2.03$. Therefore it is quite possible that the extra signal in the spectrum of HP_{ox} from *Chromatium* is related to the weak signal at $g = 2.01$ seen in the spectrum of oxidized bacterial ferredoxin from sources such as *Cl. pasteurianum* [40] and *Cl. acidi-urici*.[41] If so then the model discussed here predicts a ground state for the oxidised cluster $[Fe_4S_4(S\text{–}R)_4]^-$ as the E'' spinor component of a ^2E tetrahedral state with the g factors given by the expression in equation (13). We are currently investigating the presence of multiple magnetic species in iron–sulphur clusters using ultra-low-temperature magnetic circular dichroism spectroscopy.

APPENDIX

Evaluation of Matrix Elements of L.—In the calculation of g factors we require to evaluate matrix elements of L, the orbital angular momentum operator within and between the orbital subsystems shown in Table 1. These are necessary both for the estimation of Zeeman energies and for the evaluation of matrices of the spin–orbit coupling operator. It turns out to be a particularly tedious problem in the case of a tetrahedral cluster.

The first stage is to make the co-ordinates of the operator and the wavefunctions compatible. The orbital angular momentum operators $L_x^{(0)}$, $L_y^{(0)}$, and $L_z^{(0)}$, in co-ordinates X_0, Y_0, and Z_0 located at the centre of the tetrahedron, can be expressed in terms of co-ordinate systems on the individual metal atoms using standard transformation matrices. The results are summarised in Table 5.

Because of the complexity of these expressions some simplifying assumptions are necessary for the calculation of the matrix elements. Terms involving $a(\partial/\partial x_i)$ and $a(\partial/\partial y_i)$ do not appear in any expressions due to their cancellation on account of opposing signs. We do, however, choose to ignore overlap integrals between orbitals on different centres so that our final matrix elements are independent of the size of the metal cluster and of its overall oxidation state. It can be shown that the contributions from the angular momentum on the local centres far outweighs in magnitude the contribution from overlap terms. We carried out a specimen calculation retaining overlap terms and found that the overlap terms contributed *ca.* 0.02—0.03

TABLE 5

Relationships between orbital angular momentum operators expressed in co-ordinates X_0, Y_0, and Z_0 based at centre of tetrahedron $[l_{z_i}^{(0)}]$ and in local co-ordinates, x_i, y_i, z_i, where i = 1—4, at metal atoms. a is the distance of the metal atom from the centre of the tetrahedron. Where more than one sign is shown in an equation the signs are to be read from top to bottom as i has the value 1—4

$$L_{Z_0} = \sum_{i=1}^{4} l_{z_i}^{(0)}$$

$$l_{z_i}^{(0)} = \begin{matrix}-\\+\end{matrix}\frac{1}{\sqrt{3}} l_{z_i} + \frac{1}{\sqrt{3}} l_{z_i} + i\hbar\sqrt{2}\, a \frac{\partial}{\partial y_i}$$

$$L_{X_0} = \sum_{i=1}^{4} l_{x_i}^{(0)}$$

$$l_{x_i}^{(0)} = \begin{matrix}-\\+\end{matrix}\frac{1}{\sqrt{6}} l_{x_i} \begin{matrix}+\\-\end{matrix}\frac{1}{\sqrt{2}} l_{y_i} \begin{matrix}-\\+\end{matrix}\frac{1}{\sqrt{3}} l_{z_i} \begin{matrix}-\\+\end{matrix} i\hbar a\left(\frac{\sqrt{3}}{\sqrt{2}}\frac{\partial}{\partial x_i} + \frac{1}{\sqrt{2}}\frac{\partial}{\partial y_i}\right)$$

$$L_{Y_0} = \sum_{i=1}^{4} l_{y_i}^{(0)}$$

$$l_{y_i}^{(0)} = \begin{matrix}-\\+\end{matrix}\frac{1}{\sqrt{6}} l_{x_i} \begin{matrix}-\\+\end{matrix}\frac{1}{\sqrt{2}} l_{y_i} \begin{matrix}+\\-\end{matrix}\frac{1}{\sqrt{3}} l_{z_i} \begin{matrix}+\\-\end{matrix} i\hbar a\left(\frac{\sqrt{3}}{\sqrt{2}}\frac{\partial}{\partial x_i} - \frac{1}{\sqrt{2}}\frac{\partial}{\partial y_i}\right)$$

$i\hbar$ when $\rho = 7.0$ compared with the single centre term of 0.5 $i\hbar$. We therefore decided not to retain these terms in our final calculation.

With these approximations the values obtained are given in Table 6 for L_z only.

TABLE 6

Evaluation of matrix elements of L_z for the subsets of molecular orbitals $|X^2 - Y^2, XY|$ and $|XZ, YZ|$ given in Table 1

$|X^2 - Y^2, XY|$

$$\langle t_1 Y|L_z|t_1 X\rangle = -i\hbar$$
$$\langle t_2 YZ|L_z|t_2 XZ\rangle = +i\hbar$$

$|XZ, YZ|$

$$\langle t_1 Y|L_z|t_1 X\rangle = +\frac{i\hbar}{2}$$
$$\langle t_2 YZ|L_z|t_2 XZ\rangle = -\frac{i\hbar}{2}$$

[0/1586 *Received*, 17*th October*, 1980]

REFERENCES

[1] For a series of reviews see ' Iron–Sulfur Proteins,' ed. W. Lovenberg, Academic Press, New York, 1977, vol. 3.

[2] C. W. Carter, J. Kraut, S. T. Freer, R. A. Alden, L. C. Sieker, E. Adman, and L. H. Jensen, *Proc. Natl. Acad. Sci. U.S.A.*, 1972, **69**, 3526.

[3] R. Cammack, *Biochem. Biophys. Res. Commun.*, 1973, **54**, 548.

[4] R. Cammack, D. P. E. Dickson, and C. E. Johnson, in ref. 1.

[5] R. H. Holm, *Acc. Chem. Res.*, 1977, **10**, 427.

[6] D. V. DePamphilis, B. A. Averill, T. Herskovitz, L. Que, jun., and R. H. Holm, *J. Am. Chem. Soc.*, 1974, **96**, 4159.

[7] W. H. Orme-Johnson and R. H. Sands, in ' Iron–Sulfur Proteins,' ed. W. Lovenberg, Academic Press, New York, 1973, vol. 2, ch. 5.

[8] B. C. Antanaitis and T. H. Moss, *Biochim. Biophys. Acta*, 1975, **405**, 262.
[9] P. J. Stephens, A. J. Thomson, T. A. Keiderling, J. Rawlings, K. K. Rao, and D. O. Hall, *Proc. Natl. Acad. Sci. U.S.A.*, 1978, **75**, 5273.
[10] P. J. Stephens, A. J. Thomson, J. B. R. Dunn, T. A. Keiderling, J. Rawlings, K. K. Rao, and D. O. Hall, *Biochemistry*, 1978, **17**, 4770.
[11] M. K. Johnson, A. J. Thomson, A. E. Robinson, K. K. Rao, and D. O. Hall, *Biochim. Biophys. Acta*, in the press.
[12] A. J. Thomson, *Biochem. Soc. Trans.*, 1975, **3**, 468.
[13] C. Y. Yang, K. H. Johnson, R. H. Holm, and J. G. Norman, jun., *J. Am. Chem. Soc.*, 1975, **97**, 6596.
[14] M. B. Robin and P. Day, *Adv. Inorg. Chem. Radiochem.*, 1967, **10**, 247.
[15] R. B. Frankel, B. A. Averill, and R. H. Holm, *J. Phys. (Paris)*, 1974, **35**, 66—107.
[16] D. P. E. Dickson, C. E. Johnson, R. Cammack, M. C. W. Evans, D. O. Hall, and K. K. Rao, *Biochem. J.*, 1974, **139**, 105.
[17] R. N. Mullinger, R. Cammack, K. K. Rao, D. O. Hall, D. P. E. Dickson, C. E. Johnson, J. D. Rush, and A. Simonopoulous, *Biochem. J.*, 1975, **151**, 75.
[18] C. L. Thompson, C. E. Johnson, D. P. E. Dickson, R. Cammack, D. O. Hall, U. Weser, and K. K. Rao, *Biochem. J.*, 1974, **139**, 97.
[19] E. J. Laskowski, J. G. Reynolds, R. B. Frankel, S. Foner, G. C. Papaefthymiou, and R. H. Holm, *J. Am. Chem. Soc.*, 1979, **101**, 6562.
[20] W. A. Eaton, G. Palmer, J. P. Fee, T. Kimura, and W. Lovenberg, *Proc. Natl. Acad. Sci. U.S.A.*, 1971, **68**, 3015.
[21] R. S. Gall, N. G. Connelly, and L. F. Dahl, *J. Am. Chem. Soc.*, 1974, **96**, 4022.
[22] Trinh-Toan, Boan Keng Teo, J. A. Ferguson, T. J. Meyer, and L. F. Dahl, *J. Am. Chem. Soc.*, 1977, **99**, 408.
[23] J. W. Lauher, *J. Am. Chem. Soc.*, 1978, **100**, 5305.
[24] D. J. Robbins and A. J. Thomson, *J. Chem. Soc., Dalton Trans.*, 1972, 2350.
[25] R. H. Holm and J. A. Ibers, ref. 1, ch. 7.
[26] F. A. Cotton and T. E. Haas, *Inorg. Chem.*, 1964, **3**, 10.
[27] J. S. Griffith, ' The Theory of Transition Metals,' Cambridge University Press, 1964.
[28] M. Cerdonio, R.-H. Wang, J. Rawlings, and H. B. Gray, *J. Am. Chem. Soc.*, 1974, **99**, 6534.
[29] E. J. Laskowski, R. B. Frankel, W. O. Gillum, G. C. Papaefthymiou, J. Renaud, J. A. Ibers, and R. H. Holm, *J. Am. Chem. Soc.*, 1978, **100**, 5322.
[30] R. Cammack, *Biochem. Soc. Trans.*, 1975, **3**, 482.
[31] E. Konig, in ' Physical Methods in Advanced Inorganic Chemistry,' eds. H. A. O. Hill and P. Day, Interscience, London, 1968, ch. 7.
[32] Ref. 27, p. 341.
[33] B. Bleaney, K. D. Bowers, and R. S. Trenam, *Proc. R. Soc. London, Ser. A*, 1955, **228**, 157.
[34] A. Abragam and B. Bleaney, in ' Electron Paramagnetic Resonance of Transition Ions,' Oxford University Press, 1970, ch. 21.
[35] T. Herskovitz, B. A. Averill, R. H. Holm, J. A. Ibers, W. D. Phillips, and J. F. Weiher, *Proc. Natl. Acad. Sci., U.S.A.*, 1972, **69**, 2437.
[36] W. D. Phillips, M. Poe, C.-C. McDonald, and R. G. Bartsch, *Proc. Natl. Acad. Sci., U.S.A.*, 1970, **67**, 682.
[37] R. Englman, ' The Jahn–Teller Effect in Molecules and Crystals,' Wiley–Interscience, London, 1972.
[38] R. J. Gillespie, ' Molecular Geometry,' van Nostrand Reinhold, London, 1972.
[39] H. Blum, J. C. Salerno, and M. A. Cusanovich, *Biochem. Biophys. Res. Commun.*, 1978, **84**, 1125.
[40] Ref. 7, p. 226.
[41] W. V. Sweeney, A. J. Bearden, and J. C. Rabinowitz, *Biochem. Biophys. Res. Commun.*, 1974, **59**, 188.